The Application of Low-Temperature Thermochronology to the Geomorphology of Orogenic Systems

19

Taylor F. Schildgen and Peter A. van der Beek

Abstract

The geomorphologic evolution of orogens has been a subject of revived interest and accelerated development over the past few decades, thanks to both the increasing availability of high-resolution data and computing power and the realisation that orogenic topography plays a central role in coupling deep-earth and surface processes. Low-temperature thermochronology takes a central place in this revived interest, as it allows us to link quantitative geomorphology to the spatial and temporal patterns of exhumation. In particular, rock cooling rates over million-year timescales derived from thermochronological data have been used to reconstruct rock exhumation histories, to detect km-scale relief changes, and to document lateral shifts in relief. In this chapter, we review how classic approaches of determining exhumation histories have contributed to our understanding of landscape evolution, and we highlight novel approaches to quantifying relief changes that have been developed over the last decade. We discuss how patterns of exhumation in laterally accreting orogens are recorded by low-temperature thermochronology, and how such data can be applied to infer temporal variations in exhumation rates, providing indirect constraints on topographic development. We subsequently review recent studies aimed at quantifying relief development and modification associated with river incision, glacial modifications of landscapes, and shifts in the position of range divides. We also point out how interpretations of some datasets are non-unique, emphasizing the importance of understanding

the full range of processes that may influence landscape morphology and how each may affect spatial patterns of thermochronologic ages.

19.1 Introduction

Understanding the development of topography not only helps to reconstruct the geodynamic and surface processes responsible for landscape development, but it is also one of the most important requirements for correctly interpreting stratigraphic records, speciation patterns, and regional to global paleoclimatic changes (Ruddiman 1997; Crowley and Burke 1998). Despite its clear importance, some of the most common techniques for reconstructing paleotopography, involving reconstructing changes in paleotemperature from paleobotany or changes in stable-isotope ratios, have limited resolution, and the latter in particular require detailed knowledge of air circulation patterns, isotope lapse rates in space and time, continental (evapo-) transpiration, and vapor recycling (Mulch 2016). Moreover, although these approaches can help reveal the existence of high topography, they typically do not provide information on the distribution of elevation across the landscape (i.e., the relief), such as may be created by rivers or glaciers. Low-temperature thermochronology complements and may offer some advantages over these approaches. Although it does not provide direct constraints on paleo-elevations, low-temperature thermochronology can be used to (1) resolve changes in rock cooling rates over million-year timescales, which can be interpreted in terms of rock exhumation and may provide indirect constraints on topographic development (e.g., Montgomery and Brandon 2002); (2) detect km-scale relief changes; and (3) document lateral shifts in relief.

One of the most common applications of low-temperature thermochronology in the realm of geomorphology has been to test for changes in erosion/exhumation rates, which are typically linked to changes in climate, uplift rates, and/or

T. F. Schildgen (✉)
Helmholtz Zentrum Potsdam, GeoForschungsZentrum (GFZ), Potsdam, Germany
e-mail: tschild@gfz-potsdam.de

P. A. van der Beek
Institut des Sciences de la Terre (ISTerre), Université Grenoble Alpes, Grenoble, France

topography. But changes in exhumation rates are typically linked to changes in topographic relief, making it difficult to separate the two. Although the influence of changing relief on low-temperature thermochronometers has been appreciated for decades (e.g., Stüwe et al. 1994; Mancktelow and Grasemann 1997), it is only within the past decade that a number of novel approaches to quantify changes in landscape relief have emerged. These relief changes include those associated with river incision, glacial modifications of landscapes, and shifts in the position of range divides. Because thermochronometers are typically limited to spatial resolution on the km scale and temporal resolution on the million-year scale, thermochronological data is most relevant for discerning long-term changes in relief that occur in orogenic or post-orogenic settings.

In this chapter, we review how classic approaches of determining exhumation histories have contributed to our understanding of landscape evolution, and we highlight novel approaches to quantifying relief changes. In each case, a range of different sampling schemes have provided useful information (Fig. 19.1): bedrock samples have been collected in transects that traverse topography either in very steep (Fig. 19.1b, c) or in sub-horizontal (Fig. 19.1d) transects, over distances that are either localised or span the width of an orogen. Detrital samples (Fig. 19.1e) have been collected from modern river sediments throughout the landscape and from within dated sedimentary stratigraphic sections. Previous reviews (e.g., Braun 2005; Spotila 2005; Braun et al. 2006; Reiners and Brandon 2006) have laid out the groundwork for many of these techniques; here, we will focus on studies that have taken advantage of the record of past thermal structure and erosion patterns contained in low-temperature thermochronometers to study landscape development in orogenic systems.

## 19.2 Exhumation Histories from Low-Temperature Thermochronology

On the scale of a compressional orogenic system, the tectonic (accretionary) influx of crustal material into the system leads to thickening of the crust, isostatic uplift of the surface, and increasing topographic relief. Because erosion rates tend to increase with steeper slopes (Ahnert 1970), topographic relief is predicted to increase until the flux of material leaving the system through erosion matches the tectonic influx (Jamieson and Beaumont 1988). An important refinement to this concept in orogenic settings was the notion of "threshold hillslopes," which are the strength-limited maximum slopes that can be achieved despite further increases in erosion rates related to landslide frequency (Larsen and Montgomery 2012). This concept, first illustrated by the nonlinear
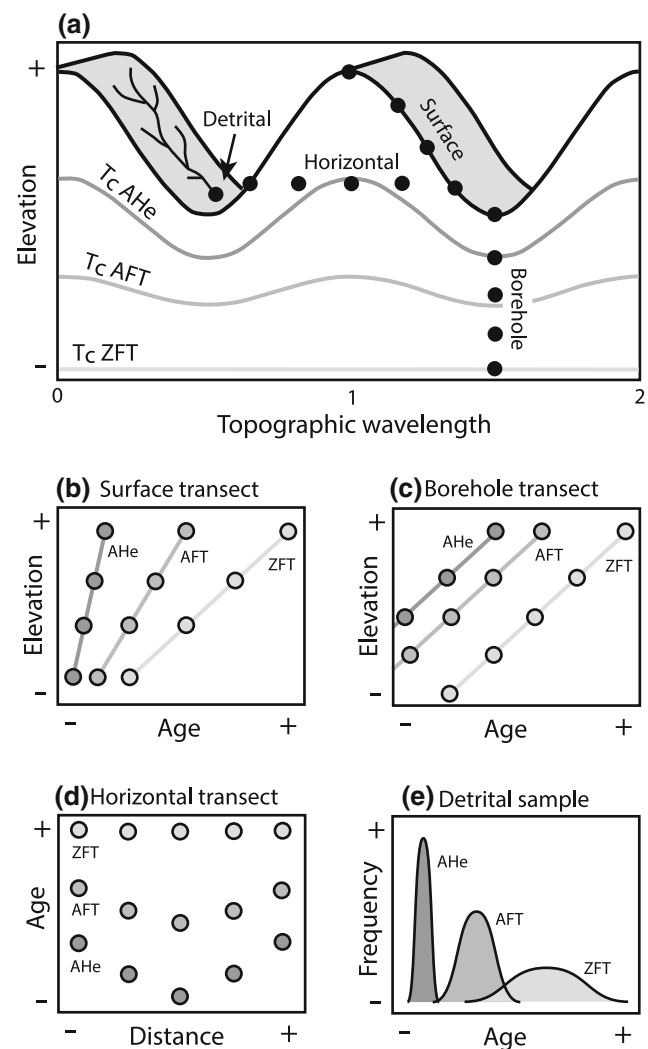
Fig. 19.1 Sampling schemes for thermochronologic data. **a** Illustration of various surface- and subsurface sampling schemes. Solid black circles are sample sites. T_c refers to closure temperature of the associated thermochronologic system. AHe: apatite (U–Th)/He; AFT: apatite fission track; ZFT: zircon fission track. **b** Age-elevation plot of a steep elevation surface transect. For the thermal structure shown in (**a**), the slope of the ZFT data provides the correct exhumation rate, while those of the AFT and AHe data overestimate the exhumation rate (see Sect. 19.2.2.2). **c** Age-elevation plot of borehole samples, in which each thermochronologic system provides the correct exhumation rate if the thermal structure is steady over time. **d** Age-distance plot of samples from a horizontal transect, which reflect the inverted shape of the T_c isotherm at the time that the samples crossed it. **e** Age-frequency plot of a detrital sample, illustrating the distribution of ages that result from material derived from a range of elevations within the source area; note that the width of the PDF is comparable to the range of ages shown in (**b**). Parts (**a–d**) modified from Braun et al. (2012), reproduced with permission from Elsevier

relationship between mean slope and erosion rates derived from thermochronological data (Burbank et al. 1996; Montgomery and Brandon 2002), has since been supported with catchment-mean erosion rates derived from cosmogenic nuclides (e.g., Binnie et al. 2007; Ouimet et al. 2009).

If the accretionary flux remains constant, topography is likely to be relatively stable as well, with steeper slopes enabling faster erosion in areas of faster rock uplift (Willett and Brandon 2002). Under these conditions, exhumation steady state, reflecting the rates and pathways through which rocks are exhumed to the surface, should also be reached (Willett and Brandon 2002) (Fig. 19.2). Hence, topographic and exhumational steady state are presumably closely linked. In the examples that follow, we will illustrate how exhumation histories derived from thermochronology data have been used to infer either steady-state topography or changes in uplift rates and the evolution of topography.
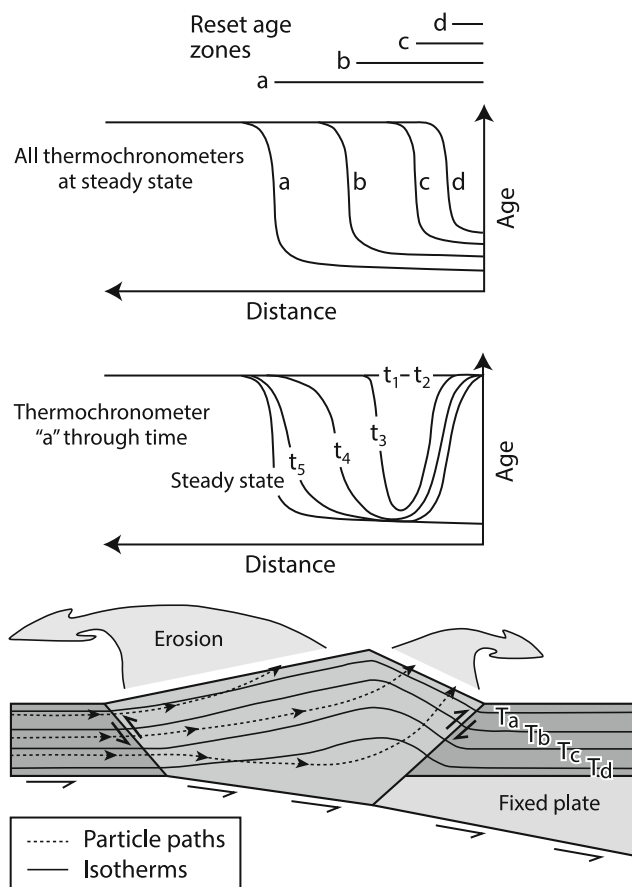
Fig. 19.2 Brandon 2002, reproduced with permission from the Geological Society of America). Closure temperature "*T*" for each thermochronometer (with subscripts a through d) is illustrated in the cartoon below. Exhumation pathways that bring samples below their respective closure isotherms result in reset ages at the surface, which are much younger than those of samples that did not pass below their closure isotherm. Note that thermochronometers with lower closure temperatures show a wider distribution of reset ages across the orogen, with reset zones of higher-temperature thermochronometers nested within

19.2.1 Exhumation Patterns in Laterally Accreting Orogens

The spatial distribution of thermochronometric ages across an orogen can help reveal whether or not exhumational steady state has been reached (Batt and Braun 1999; Willett and Brandon 2002). Material that passes through a compressional orogenic system follows a trajectory that is controlled by the direction of accretion and the pattern of erosion at the surface (Fig. 19.2). Material that enters the system through the accretionary flux will be heated to a temperature that depends on the depth of its trajectory before being cooled as it approaches the surface. Across a laterally accreting orogen, material that reached greatest depths tends to occur near the center, or is offset toward the retro side of the orogen (opposite from the accreting side) (Fig. 19.2). This characteristic of the material pathways implies that when an orogen reaches exhumational steady state (unchanging rates and patterns of exhumation), different thermochronometers will show distinct patterns of reset ages, with higher-temperature thermochronometers only reset in the region revealing deepest exhumation pathways, and lower-temperature thermochronometers showing wider zones of reset ages. Overall, this should create a pattern of higher-temperature reset age zones successively nested within lower-temperature reset age zones (Fig. 19.2).

Several studies have taken advantage of this characteristic of compressional orogenic systems to test for exhumational steady state. Batt and Braun (1999) used the pattern of nested ages in the southern Alps of New Zealand together with thermal modeling (see also Chap. 13, Baldwin et al. 2018) to illustrate the west-to-east transport of material across the orogen, as well as to show that the system is close to or at exhumational steady state. A nested pattern of ages across the Cascadia wedge in NW Washington state (Brandon et al. 1998) was argued to illustrate the existence of flux steady state, but not yet exhumational steady state, because the reset age zones have not yet reached the northeastern margin of the orogen (Batt et al. 2001). In Taiwan as well, the pattern of reset zircon (ZFT) and apatite (AFT) fission-track ages published by Liu et al. (2001) and Willett et al. (2003) was used to argue that the central portion of the mountain range is in exhumational steady state. However, because the collision propagates to the south, steady state has not yet been reached for the entire range, leading to a narrowing and eventual disappearance of the steady-state zone to the south (Willett and Brandon 2002; Willett et al. 2003).

The importance of lateral rock advection for creating asymmetric topography and controlling exhumation pathways has been demonstrated on smaller spatial scales as well, including an individual fault-bend fold (e.g., Miller et al. 2007). Across the Himalayan front, Whipp et al. (2007) showed how

lateral rock advection with spatial variations in erosion rates was necessary to explain complex patterns of AFT data. Since then, numerous studies have used thermochronologic data from the Himalaya to reconstruct exhumation pathways across individual structures and/or ramps with duplex structures (e.g., Robert et al. 2009, 2011; Herman et al. 2010; Landry et al. 2016; van der Beek et al. 2016).

19.2.2 Determining Exhumation Histories

Although obtaining a wide spatial distribution of cooling ages is effective for evaluating the exhumational "state" of an orogen, useful information can also be derived from more spatially targeted sets of samples. In the following section, we review various approaches to deriving exhumation histories based on (i) multiple thermochronometers and shorter-term erosion rate data, (ii) age-elevation transects, and (iii) detrital thermochronology (see also Chap. 9, Fitzgerald and Malusà 2018 and Chap. 10, Malusà and Fitzgerald 2018b). It is important to keep in mind that exhumation rates derived from thermochronology are not measured directly (see Chap. 8, Malusà and Fitzgerald 2018a), but rather are inferred from cooling ages and an assumed crustal thermal structure. As such, we discuss several of the complications that can make it difficult to derive accurate exhumation rates without the aid of thermal modeling.

19.2.2.1 Exhumation Histories from Multiple Thermochronometers

As argued in Sect. 19.2, topographic and exhumational steady states are often presumed to be linked (Willett and Brandon 2002). Hence, exhumation histories derived from multiple thermochronometers have commonly been used to test for topographic steady state. Studying the Smoky Mountains (USA), Matmon et al. (2003) reconstructed an exhumation history not only with low-temperature thermochronometry, but also with cosmogenic nuclides and sediment yields to demonstrate similar exhumation rates over timescales of 10^8–10^2 years. This apparent longevity of the topography of the range was suggested to result from a thickened crustal root that has responded isostatically to erosion for nearly 200 million years (Matmon et al. 2003). However, even in the case of persistently steady exhumation in post-orogenic settings, changes in topography may occur. Within the Dabie Shan of eastern China, Reiners et al. (2003b) used AFT, ZFT and apatite (U–Th)/He data (AHe) to infer similar exhumation rates over the past ~115 million years, but the data were best predicted by assuming a decay of topography over time. Braun and Robert (2005) refined the estimates of relief loss to between a factor of 2.5–4.5 since the cessation of tectonic activity.

In many other cases, exhumation histories spanning millions of years reveal changes through time. Some of the earliest studies of exhumation histories based on multiple thermochronometers were used to infer uplift and the development of topography in the European Alps (e.g., Wagner et al. 1977; Hurford 1986; Hurford et al. 1991) and in the northwest Himalaya (e.g., Zeitler et al. 1982). However, linking an exhumation history to topographic development is not always straightforward. As we will illustrate below, even in the case of similar derived exhumation histories, differing interpretations of paleotopography can emerge.

Several studies have used exhumation histories from multiple thermochronometers to infer multi-km-uplift of the Tibetan plateau. In eastern Tibet, Kirby et al. (2002) used biotite ^{40}Ar/^{39}Ar thermochronology, multiple diffusion-domain modeling of alkali feldspar ^{40}Ar release spectra, and (U–Th)/He thermochronology of zircon (ZHe) and apatite to construct cooling histories of two different study areas, one within the Tibetan plateau interior, and another at the eastern plateau margin adjacent to the Sichuan Basin. The plateau margin site revealed very slow cooling from Jurassic to the late Miocene or early Pliocene, followed by rapid cooling. The plateau interior site, in contrast, showed relatively slow cooling throughout the same period, with only a small increase in cooling rates starting sometime within the middle Tertiary. Kirby et al. (2002) suggested that the rapid cooling along the plateau margin site was induced by the development of relief in that area, implying that the high topography adjacent to the Sichuan Basin was created in the late Miocene or early Pliocene.

A similar approach was used by van der Beek et al. (2009) in the northwest Himalaya to help determine the age and origin of high elevation, low-relief surfaces characterising that part of the orogen. By combining AFT with AHe and ZHe thermochronology, they found that the Deosai plateau, a low-relief surface at ~4 km elevation east of Nanga Parbat, had experienced relatively slow cooling since at least the middle Eocene (~35 Ma), just 15–20 Myr after the onset of India–Asia collision. They therefore inferred that the region marks one of several remnants of a plateau region that had already been uplifted by middle Eocene time. Rohrmann et al. (2012) extended the multi-thermochronometer approach into central Tibet, where they found moderate to rapid cooling from Cretaceous to Eocene time, followed by relatively slow cooling since ~45 Ma. They suggested that the early phase of rapid cooling was related to crustal shortening, thickening, and erosion associated with India-Asia collision, whereas the subsequent extended phase of slow cooling represents the establishment of a high elevation, low-relief plateau in the Eocene, in line with the interpretations of van der Beek et al. (2009).

Similar to the studies by van der Beek et al. (2009) and Rohrmann et al. (2012), Hetzel et al. (2011) found evidence for rapid cooling in south-central Tibet between ∼70 and 55 Ma followed by a phase of very slow cooling since ∼50 Ma based on AFT, ZHe, and AHe data. However, unlike the other interpretations, Hetzel et al. (2011) suggested that the slow exhumation since ∼50 Ma represented a phase of peneplanation from laterally migrating rivers at low elevations, and that uplift must have occurred sometime later, subsequent to India-Eurasia collision, without inducing any faster exhumation. Highlighting the differing assumptions that led to these very different interpretations, Rohrmann et al. (2012) argued that low-relief surfaces can form at high elevation, calling into question the suggestions of Hetzel et al. (2011). The contrasting interpretations illustrate the potential difficulty of inferring uplift and topographic development from cooling (exhumation) histories alone (see also Chap. 8, Malusà and Fitzgerald 2018a).

19.2.2.2 Exhumation Histories from Age-Elevation Relationships

In regions of high topographic relief, steep elevation transects of bedrock samples can be used to derive exhumation rates over a range of time defined by the age distribution of the samples, with the slope of the line on an age-elevation plot (for a single thermochronometer) reflecting, to a first order, the exhumation rate. Wagner and Reimer (1972) and Wagner et al. (1977) were the first to propose and apply this approach to determine exhumation histories at several locations within the European Alps. Assumptions inherent to this approach include: (1) the sample's elevation is an accurate proxy for distance from the closure-temperature (T_c) isotherm; (2) there are minimal differences in the erosion rates across the horizontal distance of the samples; and (3) the isotherm's position has not changed over the timescale of exhumation (Reiners and Brandon 2006). The first assumption is most problematic for low-temperature systems, because their associated T_c isotherms more closely mimic topography compared to high-temperature systems (Stüwe et al. 1994, Fig. 19.1a). Braun (2002a) noted that in these cases, exhumation rates estimated directly from age-elevation relationships will be overestimated, as the change in elevation from one sample to the next is greater than the change in the distance traveled from the T_c isotherm (Fig. 19.1a, b). The second assumption may be valid in cases where the horizontal distance between samples is minimal (e.g., Braun 2002a; Valla et al. 2010), as will be discussed in more detail in Sect. 19.3.1.2. The third assumption may be reasonable for areas that have undergone exhumation at constant rates.

Generally, the onset of faster exhumation will produce a region over which slopes of the age-elevation relationship change, because thermochronometers tend to exhibit a zone over which daughter products (or fission tracks) are only partially retained (or annealed) (Gleadow and Fitzgerald 1987; Baldwin and Lister 1998; Wolf et al. 1998). In the case of AHe thermochronology, this "partial retention zone" (PRZ) occurs between ∼40–80 °C for typical cooling rates, with the exact bounds dependent on the chemical composition of the crystal, the cooling rate, and any accumulated radiation damage that affects He diffusion (Reiners and Brandon 2006). In the case of AFT thermochronology, tracks that are created will be instantaneously annealed at temperatures above 110 °C, and slowly annealed within the "partial annealing zone" (PAZ) between ∼60 and 110 °C (Reiners and Brandon 2006), the exact temperatures again dependent on apatite composition and cooling rate. Hence, even in the case of a sudden increase in exhumation rates, age-elevation relationships tend to show a curved or double-kinked zone, with the zone of intermediate or changing slope representing the width of the exhumed PAZ/PRZ (see Chap. 9, Fitzgerald and Malusà 2018 for details).

Another complication to directly inferring exhumation rates from age-elevation relationships arises because isotherms tend to be advected upward with the onset of faster exhumation; hence, the onset of faster cooling (which involves rocks crossing isotherms) will be delayed. Moore and England (2001) showed that for a step-wise increase in exhumation rates, the cooling ages will initially reflect a gradual increase in exhumation rates. Reiners and Brandon (2006) estimated the time required for each isotherm to reach a steady position following the onset of faster exhumation: for an increase in exhumation rate from 0 to 1 km/Myr, the T_c isotherm for He diffusion in apatite slows to 10% of its initial (advected) upward velocity after ∼2.4 Myr, while it takes ∼7.5 Myr for the T_c isotherm of Ar in muscovite to slow to 10% of its initial velocity.

Changes in relief can also affect age-elevation relationships. Using synthetic data extracted from the finite-element thermal-kinematic model Pecube (Braun 2003), Braun (2002a) illustrated how increasing relief leads to a shallower slope of the plot, whereas decreasing relief leads to a steepening. In extreme cases, decreases in relief may even result in an inverted slope, with ages decreasing with increasing elevation (see Chap. 9, Fitzgerald and Malusà 2018). Although low-temperature thermochronometers are most sensitive to changes in relief, Braun (2002a) illustrated that age-elevation plots of all thermochronometers with T_c below 300 °C are affected by it. A complication that follows from these findings is that a change in slope in an age-elevation relationship may result from a change in relief, a change in exhumation rates, or both. In a synthetic modeling study, Valla et al. (2010) investigated how well changes in exhumation rates and landscape relief could be quantified from age-elevation relationships. They illustrated how multiple thermochronometers can be most effective in

resolving both, but in the case of AHe and AFT data (ages and track lengths), the rate of relief growth must be 2–3 times higher than the background exhumation rate in order to be quantified and precisely resolved. This limitation was illustrated with field data from La Meije Peak in the western Alps, where a combination of ZFT, AFT and AHe data was effective in constraining temporal changes in exhumation rates but not the relief history, due to the relatively high background denudation rates (van der Beek et al. 2010).

These complications related to the PRZ/PAZ, thermal response times, and changes in relief can make it very difficult to infer exhumation histories directly from age-elevation relationships. It is only since the development of 1D thermal models (Brandon et al. 1998; Ehlers et al. 2005; Reiners and Brandon 2006), spectral analyses (Braun 2002b), 3D thermal-kinematic models (Braun 2003), and linear inversion approaches (Fox et al. 2014), which can take into account many or all of these effects, that more accurate reconstructions of exhumation histories have been possible. However, in a densely sampled transect of Denali in Alaska, Fitzgerald et al. (1995) illustrated the power of combining AFT ages and track-length distributions to derive an accurate exhumation history without thermal modeling (see Chap. 9, Fitzgerald and Malusà 2018). Because fission tracks are slowly annealed (shortened) between ~ 60 and 110 °C (in the PAZ), but rapidly (instantaneously) annealed at temperatures above 110 °C, the pattern of track-length distributions can be used to reconstruct the position of the exhumed base of the fossil PAZ (110 °C isotherm). Indeed, in addition to finding a sharp steepening in slope of the age-elevation relationship below 4500 m elevation (starting at ~ 6 Ma), Fitzgerald et al. (1995) found a change from a wide distribution of track lengths above 4500 m (13.2 $\pm$ 2.4 μm), indicating relatively slow cooling and annealing through the PAZ, to a narrow distribution of long track lengths below 4500 m (14.6 $\pm$ 1.4 μm), indicating rapid cooling through the PAZ with minimal annealing. Hence, they identified the sharp break in slope and change in track-length distributions as the exhumed base of the fossil PAZ, which marked the 110 °C isotherm prior to the onset of rapid uplift. By reconstructing the current depth of the 110 °C isotherm based on an assumed geothermal gradient and using independent (sedimentary) constraints on the paleotopography, Fitzgerald et al. (1995) were able to infer the total rock uplift, the amount of surface uplift, as well as the amount of exhumation that occurred since the start of rapid exhumation.

19.2.2.3 Detrital Sediment Lag-Times and Age Distributions

Detrital material, either from modern river networks or from sedimentary rocks, can also be used to constrain exhumation rates across the contributing source area. One common application is to convert the difference between cooling ages and depositional ages (the "lag-time") into an exhumation rate (e.g., Brandon and Vance 1992; Brandon et al. 1998; Garver et al. 1999). Assumptions underlying this approach are discussed in Chap. 10 (Malusà and Fitzgerald 2018b). Within a single detrital sample, however, there is a range of ages, which record spatial variations in exhumation rates across the contributing area and/or topographic relief, which is typically characterized by increasing ages at higher elevations even for uniform exhumation rates (Garver et al. 1999, Fig. 19.1e). As such, a maximum exhumation rate may be determined for the youngest age population within a sample, based on the T_c isotherm depth beneath the lowest elevation point within the contributing area. In cases where multiple samples from a stratigraphic section are available, it is possible to evaluate how the lag-times, or exhumation rates, evolve through time (see Chap. 15, Bernet 2018). These patterns have been linked to the topographic evolution of orogens, with decreasing lag-times representing orogenic growth, stable lag-times representing steady state, and increasing lag-times representing topographic decay (e.g., Bernet and Garver 2005).

In an early application to the European Alps, Bernet et al. (2001) found that the ZFT grain-age distributions from a stratigraphic section spanning the last 15 Myr showed constant lag-times, suggesting steady-state exhumation since at least 15 Ma. What remained unclear, however, was how well the approach could resolve exhumation-rate changes that might have occurred. In a more recent study from the Western Alps, Glotzbach et al. (2011b) found constant AFT lag-times since 10 Ma. From their sensitivity analysis based on 3D thermal modeling with Pecube, they illustrated that the data should have been capable of resolving a twofold increase in exhumation rates at 5 Ma, but not an increase as recent as 1 Ma.

In an alternative approach, Brewer et al. (2003) and Ruhl and Hodges (2005) used the age distribution from a modern detrital sample and measurements of modern catchment relief to determine a catchment-averaged erosion rate in the Nepalese Himalaya. In essence, they use the detrital data to predict a vertical distribution of cooling ages. Both studies point out the range of assumptions inherent to the approach, including vertical exhumation pathways, steady and uniform erosion over the T_c interval represented by the detrital ages, and no change in catchment relief compared to the present. This approach is also affected by the variable mineral fertility in different source rocks, which is the variable propensity of different parent rocks to yield detrital grains of specific minerals when exposed to erosion (Malusà et al. 2016; see also Chap. 7, Malusà and Garzanti 2018). Brewer et al. (2003) used a modeling approach to explore what average erosion rate gives an age distribution most similar to the catchment hypsometry and found that good matches

could be obtained for a slowly eroding catchment. Poorer results were obtained from a more rapidly eroding catchment, which they suggested was a consequence of higher uncertainties in the younger ages, the steeper age-elevation relationship (leading to less spread in expected ages), and non-uniform erosion rates. Ruhl and Hodges (2005) simply divided the range of modern elevations by the range of ages to determine an average erosion rate, but compared the age distribution to the shape of catchment hypsometries as a first-order test for the steady-state assumptions. Out of their three studied catchments, only one showed similarity between detrital age distribution and catchment hypsometry, suggesting steady, uniform erosion over the age range of the samples (between 11 and 2.5 Ma). For the others, Ruhl and Hodges (2005) suggested that a single detrital sample was unlikely to fully characterize the temporally and spatially transient erosion of the source area.

More recent studies have incorporated significant improvements in these approaches. For example, Brewer and Burbank (2006) used a kinematic and thermal model to better predict bedrock cooling ages along the Himalayan front in central Nepal, where lateral rock advection is an important component of exhumation pathways. Furthermore, Avdeev et al. (2011) illustrated how Bayesian statistics and the Markov chain Monte Carlo algorithm could be used to invert for the timing of erosion-rate changes. When applying this approach to single-grain AFT and AHe ages from large rivers along the southeast margin of the Tibetan plateau, Duvall et al. (2012) found that all the rivers recorded an increase in exhumation rate between 11 and 4 Ma.

19.3 Relief Development and Modification in Landscapes

Although testing for changes in exhumation rates in an active orogen is one way to indirectly constrain paleotopography or paleorelief, a number of novel approaches in thermochronology have provided more direct constraints on the timing and magnitude of relief change. Most of these approaches take advantage of the tendency of near-surface isotherms to mimic the shape of topography, with strong changes in the shape of the isotherms resulting from changes in surface morphology (Fig. 19.1) (Stüwe et al. 1994; Mancktelow and Grasemann 1997). Because these effects are strongest for isotherms that are closest to the surface, most of these studies employ systems with very low T_c such as AHe or $^4He/^3He$ thermochronometry. In the subsections that follow, we explore a number of different approaches that have been used to investigate changes in landscape relief in various contexts: fluvial landscapes, glacial landscapes, and along drainage divides. As these examples show, (very) low-temperature thermochronology data have the potential to constrain models of landscape evolution when collected using a targeted sampling strategy. However, careful consideration of all possible scenarios as well as the detailed kinetic behavior of the samples is required to discriminate among competing models.

19.3.1 Relief Changes in Fluvial Landscapes

The timing and magnitude of km-scale river-valley incision can provide critical information on the influence of climatic or tectonic forcing on a landscape, or may alternatively record a major change in a river network, such as a large capture event. In the following examples, we highlight various approaches that have successfully constrained the relief history of fluvial landscapes, individual valleys, or individual reaches of a river channel.

19.3.1.1 Landscape Relief Derived from Sub-horizontal Transects

One of the earliest applications of a single thermochronometer to constrain both the magnitude and age of topographic relief within a fluvially sculpted landscape is the work by House et al. (1997, 1998, 2001) in the Sierra Nevada, California. In their approach, samples were collected at a similar elevation along the full length of the range (similar to the sampling approach illustrated in Fig. 19.1c), with the presumption that variations in age would reflect deflection of the T_c isotherm at the time the samples passed through it, and hence, paleorelief. AHe ages across the northern sector of the Sierra Nevada (the Kings and San Joaquin river valleys) ranged from ~40 to ~70 Ma and, interestingly, showed a pattern of ages that varied inversely with the long-wavelength topography of the range: older ages occurred across the broad valleys and younger ages occurred around the peaks. Accordingly, House et al. (1997, 1998, 2001) inferred that km-scale topographic relief must have existed at ~70–40 Ma.

While the existence of significant paleorelief was well demonstrated with the AHe data of House et al. (1998, 2001), later work has modified some details of the original interpretations. Braun (2002b) found from a spectral analysis of the available data that relief has decreased by at least ~50% since the end of the 70–80 Ma Laramide Orogeny, although he noted that the data points were not ideally spaced for an accurate reconstruction of relief. In contrast, Clark et al. (2005a) suggested a paleo-range crest elevation of only ~1.5 km during the Late Cretaceous (i.e., less than today's ~4 km crest elevation), which they justified by noting that river profiles, as well as increased river incision rates between 2.7 and 1.4 Ma (Stock et al. 2004), indicate two periods of renewed uplift and relief generation since ~32 Ma. In a more detailed interpretation of the

thermochronology data using Pecube thermal-kinematic modeling, McPhillips and Brandon (2012) suggested an alternative interpretation that potentially resolves the debate: Their results indicate that relief and elevations were likely high in the Late Cretaceous, decreased throughout the Paleogene, and then increased again during the Neogene. This work nicely illustrates that while direct investigations into relief development may provide better constraints on paleotopography, thermal modeling is often needed to explore the full range of possible interpretations.

19.3.1.2 Canyon Incision

On a more local scale, numerous approaches have been used to determine the incision history of an individual canyon, including dating volcanic flows and travertine deposits (e.g., Pederson et al. 2002; Thouret et al. 2007; Karlstrom et al. 2007; Montero-López et al. 2014), cave fluvial sediments (e.g., Stock et al. 2004; Haeuselmann et al. 2007), and carbonate deposits (e.g., Polyak et al. 2008), or by investigating changes in sedimentology (e.g., Blackwelder 1934; Lucchitta 1972; Wernicke 2011). Volcanic flows are useful geomorphic markers, but their ages provide only a minimum constraint on the time that a canyon was carved to the depth at which the flow is preserved; the relief may have been carved earlier, and the flow itself may not have reached the lowest elevations of the canyon. Cave deposits stranded along the banks of an incising river are mainly limited by the requirement that one must have a clear understanding of the hydrology (and paleo-hydrology) of the area to accurately relate the end of carbonate or fluvial-sediment deposition to river incision (e.g., Polyak et al. 2008; Karlstrom et al. 2008). Finally, sedimentology can be very effective for revealing changes in provenance and potentially changes in river flow regime, which could record capture events or incision in some cases (e.g., Wernicke 2011), but does not allow for direct reconstructions of incision magnitudes or rates.

Low-temperature thermochronology has provided an effective alternative (or complementary) approach in several areas. In principle, km-scale valley incision will locally depress near-surface isotherms, which can be recorded as localised, rapid cooling from low-temperature thermochronology (Schildgen et al. 2007, Fig. 19.3a). The earliest application of this approach was in Eastern Tibet, where rivers have incised more than 2 km beneath a low-relief regional surface (Fig. 19.3b). Clark et al. (2005b) compiled AHe data from several short elevation transects and interpreted the incision history after plotting the cooling ages versus depth beneath the regional surface. This approach is preferable to plotting all the samples on an age-elevation plot, because considering their broad spatial distribution, the shape of the T_c isotherm on a regional scale is best represented by the long-wavelength topography, i.e., the regional low-relief surface. Distance from the low-relief surface

therefore provides a better proxy for distance from the T_c isotherm compared to elevation, which inherently assumes that the isotherm is horizontal. Building on this work, AHe and ZHe data from the Dadu, Yalong, and upper Yangtze rivers along the Eastern Tibet margin were shown by Ouimet et al. (2010) to all reveal relatively rapid incision since between ~10 and 15 Ma, with variations in the onset suggested to be related to local upper-crustal deformation patterns superimposed on long-wavelength, epeirogenic uplift (Fig. 19.3b). Yang et al. (2016) found similar pulses of incision at or after ~6 Ma in the Mekong and Salween rivers farther to the southwest (Fig. 19.3b). They suggested that spatiotemporal variations in erosion histories, and particularly the northward temporal progression of maximum erosion rates along the Salween river, could be related to deformation associated with the northward migration of the corner of the Indian continent.

A similar approach was taken in southern Peru to constrain the incision history of the Cotahuasi-Ocoña canyon across the western margin of the central Andean plateau (Schildgen et al. 2007, 2009). In this case, plotting samples on a plot of age versus depth below a preexisting low-relief surface was critical, because the samples were collected over a very limited elevation range along a valley bottom, but over a large range of depths beneath the regional low-relief surface (Schildgen et al. 2007). Indeed, samples that were collected later from elevation transects up the canyon walls revealed a similar pattern as the valley-bottom transect on an age-depth plot (Schildgen et al. 2009). Three-dimensional thermal-kinematic modeling pointed to an onset of incision between ~8.5 and 11 Ma (Schildgen et al. 2009).

The Grand Canyon of the Colorado River has been another main target of river-incision studies based on thermochronology. Flowers et al. (2008) used AHe data from both plateau-surface and canyon-interior samples to try to distinguish between regional unroofing and canyon incision events. At the eastern end of the Grand Canyon, cooling ages ranging from ~25 to 20 Ma argued for a Late Cenozoic (post-6 Ma) phase of canyon incision below the modern plateau surface (Flowers et al. 2008). However, Early Cenozoic thermal histories from samples separated by 1500 m of elevation and stratigraphic position in the same area are very similar. This finding implies that there must have been km-scale relief at that time, most likely carved into units that have since been removed through regional unroofing; otherwise, the deeper samples would have experienced higher temperatures compared to the shallower samples (Flowers et al. 2008). Later analyses using apatite ^{4}He/^{3}He thermochronology on canyon samples corroborated this multi-phase cooling history of the eastern Grand Canyon, which contrasts with the evidence for a single-phase, Laramide cooling history of most (70–80%) of the western Grand Canyon (Flowers and Farley 2012). Earlier AFT
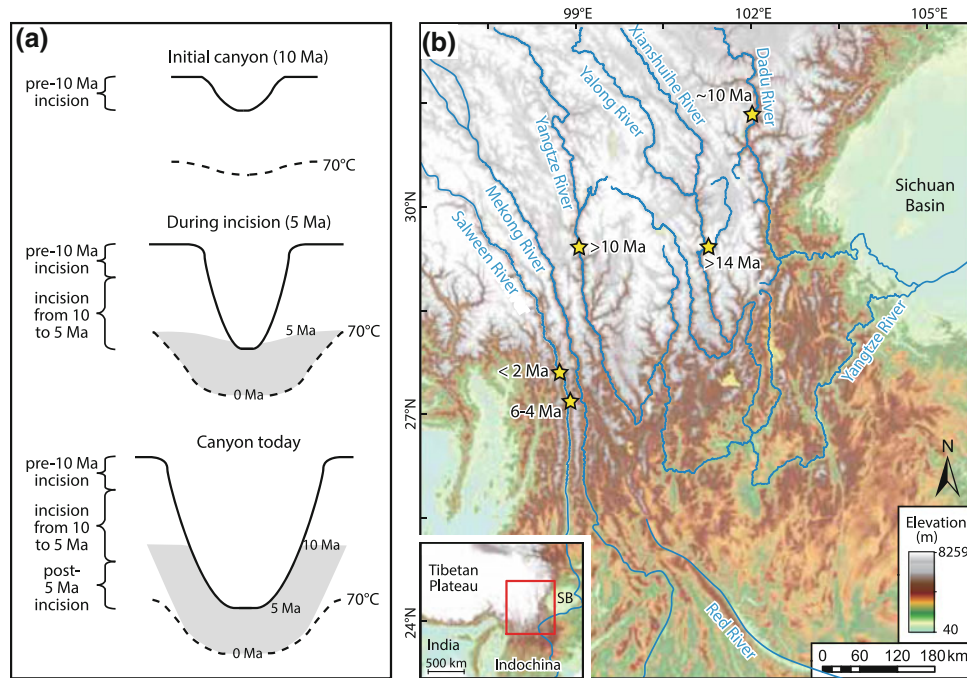
Fig. 19.3 Thermochronologic approach to constraining canyon incision history. **a** Schematic illustration of changes in topography, position of the T_c isotherm of the AHe system (70 °C), and development of a rapidly cooled zone beneath a canyon (shaded). Cartoon illustrates a scenario in which moderate relief exists prior to 10 Ma, the onset of rapid incision is at 10 Ma, and continues to the present (modified from Schildgen et al. 2007, reproduced with permission from the Geological Society of America). **b** Timing of the onset of rapid incision for rivers at various sites throughout eastern Tibet, based on thermochronometric data and modeling from Clark et al. (2005b), Ouimet et al. (2010), and Yang et al. (2016). Extent of (**b**) is outlined with red box in the inset map. SB: Sichuan Basin

studies from both the western outlet of the Grand Canyon (Fitzgerald et al. 2009) and along the eastern end of the canyon near Grand Canyon Village (Dumitru et al. 1994) also found evidence for rapid Laramide cooling. Nonetheless, the proposed Laramide incision of most of the western Grand Canyon was met with controversy. Fox and Shuster (2014) pointed out that with the uncertainties concerning how burial reheating affects the diffusion kinetics of He in apatite, it was not possible to use the data of Flowers and Farley (2012) to distinguish between the different incision scenarios. Others had argued that most of the incision in the western canyon occurred much later: Evidence pointing to post-6 Ma incision included dated volcanic flows, other thermochronology data, and the lack of Grand Canyon sediments found at its western outlet prior to 6 Ma (Karlstrom et al. 2008). But it is important to keep in mind that the high incision rates inferred from volcanic flows and speleothems represent maximum incision rates, and the lack of sediments to the west prior to 6 Ma could be explained by drainage reversal (from east- to west-flowing) at ∼6 Ma (Wernicke 2011). While the idea of some Laramide paleo-relief in the region appears to be well established, the canyon may only have become fully integrated and comparable to the modern system in the last 5–6 Ma (Karlstrom et al. 2014). Although the interpretations appear to be converging on a story of geomorphologic evolution that is consistent with the available data, the controversy surrounding this problem illustrates the importance of appreciating the limits to each approach of constraining the evolution of landscape relief.

19.3.1.3   Knickpoint Migration

When attempting to interpret river-incision data in the context of external forcing, it is important to consider potential lags in the onset of incision. In a simple case of a regional tilting of the landscape, the entire length of a river may start to incise at a similar time, close to the timing of tilting (Fig. 19.4a Scenario 1) (e.g., Braun et al. 2014). However, following a uniform increase in uplift rates or a drop in base level, a river may not immediately start incising along its full length. Instead, incision will initiate at its downstream end and propagate upward through time, with a knickpoint separating the lower, incised reach from the upper, relict reach (Whipple and Tucker 1999, Fig. 19.4a Scenario 2). Bedrock river terraces can be useful for reconstructing river incision (e.g., Burbank et al. 1996) and potentially knickpoint migration (Harkins et al. 2007), but when considering km-scale incision waves or incision histories spanning millions of years, low-temperature thermochronology may provide more insights.
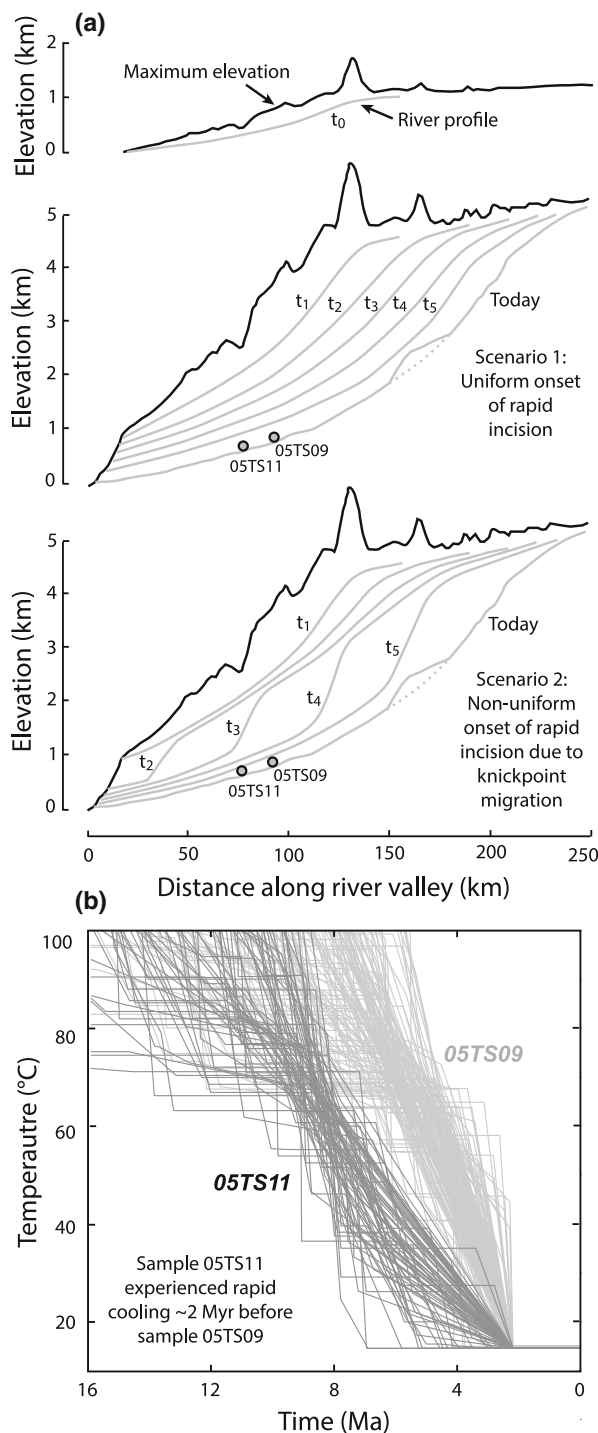
Fig. 19.4 Knickpoint propagation in the Cotahuasi Canyon (southwest Peru) from apatite $^4He/^3He$ thermochronometry (Schildgen et al. 2010, reproduced with permission from Elsevier). **a** Schematic illustration of how the river profile may evolve through time following surface uplift, either through a uniform onset of incision following monoclinal warping (Scenario 1) or upstream propagation of a knickpoint following block uplift (Scenario 2). **b** Temperature–time paths that provide good fits to $^4He/^3He$ data (see Schildgen et al. 2010 for details) illustrate the time-transgressive nature of the onset of rapid cooling for different samples collected along the valley bottom, indicating that Scenario 2 is more likely

Apatite $^4He/^3He$ thermochronometry is a promising technique for this particular application, due to its ability to resolve cooling histories at and below the He T_c (Shuster and Farley 2004, 2005). Schildgen et al. (2010) derived cooling histories from inverse modeling of apatite $^4He/^3He$ data for four different samples along the length of the canyon, in order to decipher the onset of rapid cooling in each sample. A comparison of the time-temperature paths illustrated the time-transgressive nature of the onset of rapid cooling; downstream samples showed a 1–2 Myr earlier onset of cooling compared to upstream samples, which likely represents the upstream migration of a major knickpoint (Schildgen et al. 2010, Fig. 19.4b).

19.3.2 Relief Changes in Glacial Landscapes

Glacial erosion of river valleys represents a special case of relief development. Due to the localised erosion along the lower flanks of the valley during this type of relief modification (from V- to U-shaped valley morphology, Fig. 19.5a), both spatial and temporal changes in erosion rates would be expected. However, these changes may only be resolvable with the lowest-temperature thermochronometers.

In the extensively glaciated Coast Mountains of British Columbia, Shuster et al. (2005) used apatite $^4He/^3He$ thermochronometry to resolve the onset of incision-related cooling in a steep transect of samples along a valley wall. Not only did all of the samples reveal increased cooling rates at ∼1.8 Ma, but the highest sample revealed an onset of cooling that slightly predated the lower-elevation samples, illustrating the progressive nature of valley deepening. Furthermore, because a sample on the east side of the valley revealed a later onset of cooling compared to a sample at similar elevation on the west side, Shuster et al. (2005) inferred that valley widening had proceeded toward the east. In the same region, Ehlers et al. (2006) used AHe data to illustrate that the increase in exhumation appears to have extended over a wide region, with an apparent shift in the position of a major topographic divide due to widespread glacial erosion that overtopped and eroded ridgelines.

In a slightly different approach in the western Alps, Glotzbach et al. (2011a) applied inverse numerical thermal-kinematic modeling to a dense set of AFT and AHe data across and through (via a tunnel) the Mont Blanc massif. From initial 3D thermo-kinematic modeling, in which they assumed no change in relief, they found that following a period of relatively slow exhumation, the data were most consistent with a phase of rapid exhumation starting at ∼1.7 Ma. However, that scenario did not effectively predict ages from the tunnel samples. A second scenario, which was consistent with both the tunnel and the
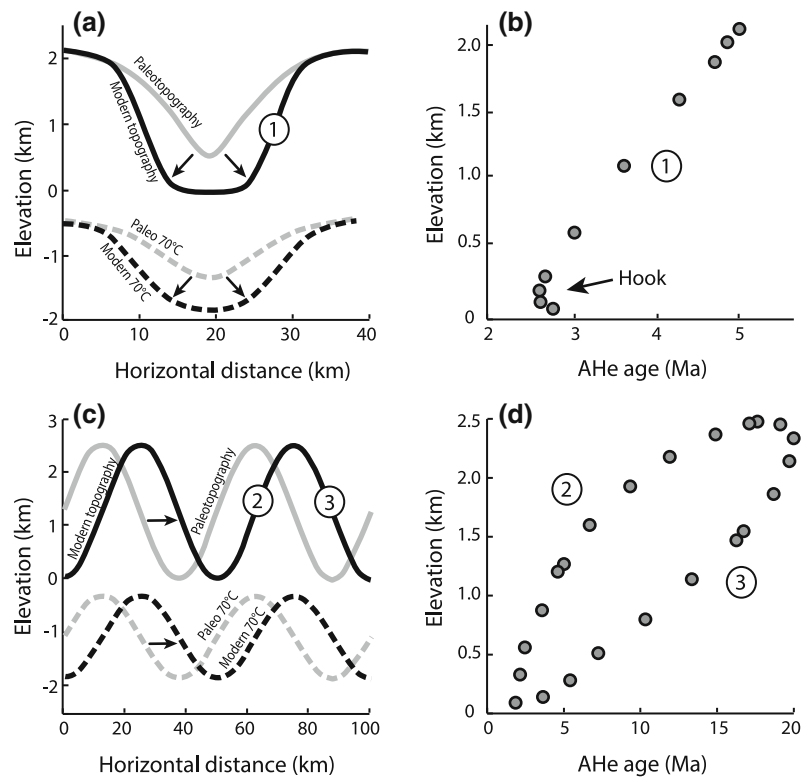
Fig. 19.5 Age-elevation transects in areas of changing relief modified from Olen et al. (2012). **a** Schematic illustration of changes in topography and position of the AHe T_c isotherm associated with increasing valley width, particularly a change from a V- to U-shaped valley. **b** Associated age-elevation transect along slope 1. **c** Illustration of changes in topography and position of the T_c isotherm associated with a lateral shift in topography, such as would be associated with asymmetric precipitation. **d** Associated age-elevation transect from the wetter (2) and drier (3) sides of the range

surface samples, included an increase in relief due to valley deepening at ∼0.9 Ma, most likely related to Alpine glaciations. AHe and ^{4}He/^{3}He data from the Rhône Valley in Switzerland combined with thermal-kinematic modeling revealed a similar pattern with even greater detail, indicating ∼1–1.5 km deepening of the glacial U-shaped valley starting at ∼1 Ma (Valla et al. 2011), representing an approximate doubling of valley relief since that time. The ∼1 Ma timing of glacial valley incision in the Alps is consistent with independent sedimentary and cosmogenic-isotope data (Muttoni et al. 2003; Haeuselmann et al. 2007) and suggests that glacial erosion only became an efficient relief-transforming agent after the mid-Pleistocene climatic transition.

In some cases, valley widening might be detectable from age-elevation transects alone. Within the Coast Ranges of British Columbia, low-temperature thermochronometers have revealed steepened (Densmore et al. 2007) or even hooked (Olen et al. 2012) patterns on age-elevation plots, with age minima occurring near the base of the valley due to focused erosion at the lower flanks (Fig. 19.5a, b). In Fig. 19.5a, this pattern can be understood by comparing the

"modern topography" to the "Paleo 70 °C" isotherm. The shortest distance between the isotherm and the modern topography, and hence, the youngest cooling ages, are found near the edges of the flattened valley bottom. Densmore et al. (2007) found that both temporal and spatial variations in erosion rates were needed to explain the pattern of thermochronometer ages in their elevation profile, but, in the absence of landscape evolution modeling, they could only qualitatively constrain the changes in relief that have occurred.

In an AHe and ^{4}He/^{3}He data set from Fiordland, New Zealand, Shuster et al. (2011) found a series of age-elevation relationships that display distinctly hooked patterns, i.e., showing a change from a positive slope higher on the valley walls to a negative slope near the base (e.g., Figure 19.5b). Using Pecube to model these data, they found that best fits to their data were achieved by models that included headward migration of km-scale topographic steps, interpreted to be facilitated by sliding-rate-dependent erosion at the base of the glaciers that carved out the landscape. Another possibility, which was not considered, is that valley widening produced or at least contributed to the distinct age-elevation

patterns. Although additional modeling is required to test if both scenarios are plausible, this example highlights the potential for non-unique interpretations of thermochronological data, particularly in the case of changing landscape relief.

19.3.3 Range-Divide Migration

In areas of asymmetric precipitation across a mountain range, a situation commonly encountered where the range strikes perpendicular to oncoming winds, both numerical (Beaumont et al. 1992; Roe et al. 2003; Anders et al. 2008) and analog (Bonnet 2009) models predict a progressive migration of the drainage divide toward the drier side of the range. In the case of spatially uniform uplift, steepening of the dry-side slopes and lowering of the wet-side slopes over the course of divide migration may eventually lead to a balance in erosion rates on both sides of the range, resulting in steady, asymmetric topography (Roe et al. 2003). Where a horizontal component to rock advection occurs, drainage divides will also tend to migrate in the direction of tectonic motion (Beaumont et al. 1992; Willett 1999; Willett et al. 2001) (Fig. 19.2). Exhumational and topographic steady state may eventually be reached, with faster tectonic deformation and exhumation occurring on the wetter, or

retrowedge (non-accreting), side (Willett 1999; Willett et al. 2001). In the former case (uniform uplift), topographic steady state will be characterized by symmetric cooling ages across the range, whereas in the latter case (with a horizontal component to uplift), topographic steady state will be characterized by asymmetric ages across the range.

However, if asymmetric ages across the range are found, the interpretation may be non-unique. Rather than reflecting a coupling between tectonic deformation and climate/erosion under steady-state topographic conditions, an asymmetric pattern of ages could reflect spatially uniform uplift with a migrating drainage divide. As Olen et al. (2012) illustrated in their modeling study, under spatially uniform uplift and asymmetric erosion, the retreating (wet) side, which erodes into the landscape faster during divide migration, is expected to yield younger ages compared to samples at a similar elevations on the advancing (drier) and more slowly eroding side (Fig. 19.5c, d). Moreover, the pattern of ages on the wet side (transect "a" in Fig. 19.5d) could mistakenly be interpreted to show an increase in exhumation rates due to the steepening of the age-elevation relationship at lower elevations.

Within the Washington Cascades (Northwestern USA, Fig. 19.6a), Reiners et al. (2003a) suggested that a spatial coincidence between peak orographic precipitation and fastest exhumation from AHe data on the western flank of the
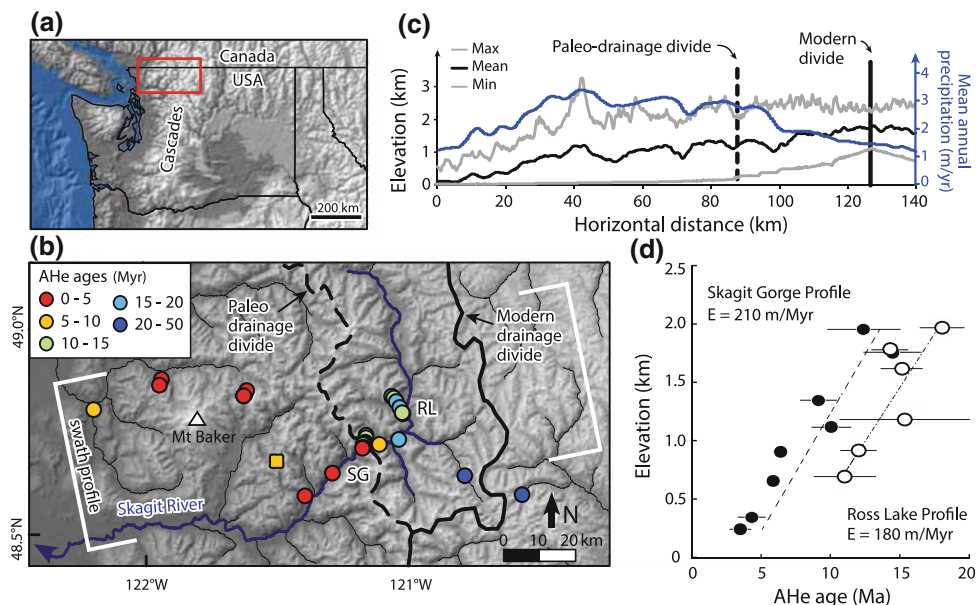
Fig. 19.6 Thermochronometric data from the Washington cascades (USA) collected over a range of mean annual precipitation values. **a** Overview of Cascades; red box outlines region shown in (**b**). **b** Sample locations colored by AHe age on digital elevation model. Samples from the Skagit Gorge (SG) elevation profile are from a wetter region on the western side of the paleo-drainage divide compared to samples from the Ross Lake (RL) profile, which is on the eastern side

of the paleo-divide. **c** Swath profile (location shown with white brackets in (**a**) shows mean, minimum, and maximum topography along the swath, and mean annual precipitation. Note the consistently younger ages on the wetter (west) side of the paleo-drainage divide, both in map view and in the age-elevation plot **d** of the two sample profiles. *E* is the exhumation rate. (**b–d**) modified from Simon-Labric et al. (2014), reproduced with permission from the Geological Society of America

range pointed to a strong coupling between climate and erosion. They noted that if topography is at or near steady state, the data would argue also for a coupling among climate, erosion, and tectonic deformation. However, denudation rates derived from cosmogenic [10]Be, which average over the past several millennia, are about four times higher than the million-year timescales, implying that the topography is not in steady state (Moon et al. 2011). A study by Simon-Labric et al. (2014) also emphasised the transient nature of topography in the area: the existence of wind gaps, drainage basins oriented parallel to the crest of the divide, and peaks in topography that are offset from the drainage divide point to a relatively recent reorganisation of the drainage system. Also, Simon-Labric et al. (2014) highlighted how AHe data reveal a pattern consistent with progressive divide migration: age-elevation plots show similar slopes, but ages are consistently younger on the wetter side at a given elevation compared to the drier side (Fig. 19.6b–d). Their study illustrates the importance of independent geomorphic interpretations of the landscape in cases where the interpretation of thermochronology data may be non-unique.

19.4 Summary

Thermochronology has proven to be a valuable tool in geomorphological studies for the past several decades. With the advent of thermal-kinematic modeling and high-resolution low-temperature thermochronology systems, we have moved from indirectly inferring paleotopography and relief development toward more precise and quantitative constraints on landscape morphology. Interpretations of thermochronological data, including age-elevation relationships, can be greatly improved with the incorporation of thermal-kinematic modeling, which can help to disentangle the influence of partial retention/annealing zones, transient motion of isotherms following a change in exhumation rate, and potentially also changes in relief versus changes in exhumation rates, on age patterns. The development of very low-temperature thermochronometers such as AHe and apatite ^{4}He/^{3}He is vital in providing the resolution necessary to quantify changes in relief and effectively distinguish them from changes in exhumation rates.

Detrital thermochronology has proven to be effective for characterising erosion rates, particularly when focusing on interpreting lag-times (the time lapse between the cooling age and depositional age). However, with respect to detecting relief changes, this approach has been hindered by insufficient characterization of complex (e.g., variable lithology, non-uniform erosion rates) source areas. As such, it seems to hold less potential for studying long-term changes in landscape relief, particularly for large, heterogenous catchments.

Finally, thermochronology data alone may be insufficient to resolve all types of changes in landscape relief. In the case of both valley widening and range-divide migration, steepened patterns at the base of age-elevation transects will result. Hence, a single transect of thermochronological data may be insufficient to distinguish valley widening or range-divide migration from an increase in regional exhumation rates. In such examples of major changes in landscape relief, multiple sets of sample transects coupled with geomorphological field observations will be crucial for deciphering the details of landscape evolution.

References

Ahnert F (1970) Functional relationships between denudation, relief, and uplift in large mid-latitude drainage basins. Am J Sci 268:243–263

Anders AM, Roe GH, Montgomery DR, Hallet B (2008) Influence of precipitation phase on the form of mountain ranges. Geology 36:479–482

Avdeev B, Niemi NA, Clark MK (2011) Doing more with less: Bayesian estimation of erosion models with detrital thermochronologic data. Earth Planet Sci Lett 305(3–4):385–395

Baldwin SL, Lister GS (1998) Thermochronology of the South Cyclades Shear Zone, Ios, Greece: effects of ductile shear in the argon partial retention zone. J Geophys Res 103:7315–7336

Baldwin SL, Fitzgerald PG, Malusà MG (2018) Chapter 13. Crustal exhumation of plutonic and metamorphic rocks: constraints from fission-track thermochronology. In: Malusà MG, Fitzgerald PG (eds) Fission-track thermochronology and its application to geology. Springer

Batt GE, Braun J (1999) The tectonic evolution of the Southern Alps, New Zealand: insights from fully thermally coupled dynamical modeling. Geophys J Int 136:403–420

Batt GE, Brandon MT, Farley KA, Roden-Tice M (2001) Tectonic synthesis of the Olympic Mountains segment of the Cascadia wedge using 2-D thermal and kinematic modeling of isotopic ages. J Geophys Res 106(B11):26731–26746

Beaumont C, Fullsack P, Hamilton J (1992) Erosional control of active compressional orogens. In: McClay KR (ed) Thrust tectonics. Chapman and Hall, London, pp 1–18

Bernet M (2018) Chapter 15. Exhumation studies of mountain belts based on detrital fission-track analysis on sand and sandstones. In: Malusà MG, Fitzgerald PG (eds) Fission-track thermochronology and its application to geology. Springer

Bernet M, Garver JI (2005) Fission-track analysis of detrital zircon. Rev Mineral Geochem 58(1):205–237

Bernet M, Zattin M, Garver JI, Brandon MT, Vance JA (2001) Steady-state exhumation of the European Alps. Geology 29:35–38

Binnie SA, Phillips WM, Summerfield MA, Fifield LK (2007) Tectonic uplift, threshold hillslopes, and denudation rates in a developing mountain range. Geology 35(8):743–746

Blackwelder E (1934) Origin of the Colorado river. Geol Soc Am Bull 45:551–566

Bonnet S (2009) Shrinking and splitting of drainage basins in orogenic landscapes from the migration of the main drainage divide. Nature Geosci 2:766–771

Brandon MT, Vance JA (1992) Fission-track ages of detrital zircon grains: implications for the tectonic evolution of the Cenozoic Olympic subduction complex. Am J Sci 292:565–636

Brandon MT, Roden-Tice MK, Garver JI (1998) Late Cenozoic exhumation of the Cascadia accretionary wedge in the Olympic mountains, NW Washington state. Geol Soc Am Bull 110:985–1009

Braun J (2002a) Quantifying the effect of recent relief changes on age-elevation relationships. Earth Planet Sci Lett 200:331–343

Braun J (2002b) Estimating exhumation rate and relief evolution by spectral analysis of age-elevation datasets. Terra Nova 14:210–214

Braun J (2003) Pecube: a new finite-element code to solve the 3D heat transport equation including the effects of a time-varying, finite amplitude surface topography. Computers Geosci 29:787–794

Braun J (2005) Quantitative constraints on the rate of landform evolution derived from low-temperature themrochronology. Rev Mineral Geochem 58:351–374

Braun J, Robert X (2005) Constraints on the rate of post-orogenic erosional decay from low-temperature thermochronologic data: application to the Dabie Shan, China. Earth Surf Proc Land 30 (9):1203–1225

Braun J, van der Beek P, Batt G (2006) Quantitative thermochronology: numerical methods for the interpretation of thermochronological data. Cambridge University Press, Cambridge, p 258

Braun J, Guillocheau F, Robin C, Baby G, Jelsma H (2014) Rapid erosion of the southern African plateau as it climbs over a mantle superswell. J Geophys Res 119(7):6093–6112

Brewer ID, Burbank DW (2006) Thermal and kinematic modeling of bedrock and detrital cooling ages in the central Himalaya. J Geophys Res 111(B9). https://doi.org/10.1029/2004jb003304

Brewer ID, Burbank DW, Hodges KV (2003) Modelling detrital cooling-age populations: insights from two Himalayan catchments. Basin Res 15(3):305–320

Burbank DW, Leland J, Fielding E, Anderson RS, Brozovic N, Reid MR, Duncan C (1996) Bedrock incision, rock uplift and threshold hillslopes in the northwestern Himalayas. Nature 379:505–510

Clark MK, Maheo G, Saleeby J, Farley KA (2005a) The non-equilibrium landscape of the southern Sierra Nevada, California. GSA Today 15(9):4–10

Clark MK, House MA, Royden LH, Whipple KX, Burchfiel BC, Zhang X, Tang W (2005b) Late Cenozoic uplift of southeastern Tibet. Geology 33(6):525–528

Crowley TJ, Burke KC (eds) (1998) Tectonic boundary conditions for climate reconstructions. Oxford University Press, Oxford, p 285

Densmore MS, Ehlers TA, Woodsworth GJ (2007) Effect of Alpine glaciations on thermochronometer age-elevation profiles. Geophys Res Lett 34:L02502. https://doi.org/10.1029/2006GL028317

Dumitru TA, Duddy IR, Green PF (1994) Mesozoic-Cenozoic burial, uplift, and erosion history of the west-central Colorado plateau. Geology 22(6):499–502

Duvall AR, Clark MK, Avdeev B, Farley KA, Chen Z (2012) Widespread late Cenozoic increase in erosion rates across the interior of eastern Tibet constrained by detrital low-temperature thermochronometry. Tectonics 31(3). https://doi.org/10.1029/2011tc002969

Ehlers T, Chaudhri T, Kumar S, Fuller C, Willett S, Ketcham RA, Brandon MT, Belton DX, Kohn BP, Gleadow AJW, Dunai TJ, Fu FQ (2005) Computational tools for low-temperature thermochronometer interpretation. Rev Mineral Geochem 58(1):589–622

Ehlers TA, Farley KA, Rusmore ME, Woodsworth GJ (2006) Apatite (U–Th)/He signal of large-magnitude accelerated glacial erosion, southwest British Columbia. Geology 34(9):765–768

Fitzgerald PG, Malusà MG (2018) Chapter 9. Concept of the exhumed partial annealing (retention) zone and age-elevation profiles in thermochronology. In: Malusà MG, Fitzgerald PG (eds) Fission-track thermochronology and its application to geology. Springer

Fitzgerald PG, Sorkhabi RB, Redfield TF, Stump E (1995) Uplift and denudation of the central Alaska range: a case study in the use of apatite fission track thermochronology to determine absolute uplift parameters. J Geophys Res 100(B10):20175–20191

Fitzgerald PG, Duebendorfer EM, Faulds JE, O'Sullivan P (2009) South Virgin-White Hills detachment fault system of SE Nevada and NW Arizona: applying apatite fission track thermochronology to constrain the tectonic evolution of a major continental detachment fault. Tectonics 28(2). https://doi.org/10.1029/2007tc002194

Flowers RM, Farley KA (2012) Apatite ^{4}He/^{3}He and (U–Th)/He evidence for an ancient Grand Canyon. Science 338(6114):1616–1619

Flowers RM, Wernicke BP, Farley KA (2008) Unroofing, incision and uplift history of the southwestern Colorado plateau from (U–Th)/He apatite thermochronometry. Geol Soc Am Bull 120:571–587

Fox M, Shuster D (2014) The influence of burial heating on the (U–Th)/He system in apatite: Grand Canyon case study. Earth Planet Sci Lett 397:174–183

Fox M, Herman F, Willett SD, May DA (2014) A linear inversion method to infer exhumation rates in space and time from thermochronometric data. Earth Surf Dyn 2:47–65

Garver JI, Brandon MT, Roden-Tice M, Kamp PJJ (1999) Exhumation history of orogenic highlands determined by detrital fission-track thermochronology. Geol Soc Spec Publ 154:283–304

Gleadow AJW, Fitzgerald PG (1987) Uplift history and structure of the Transantarctic mountains: new evidence from fission track dating of basement apatites in the Dry Valley area, southern Victoria Land. Earth Planet Sci Lett 82:1–14

Glotzbach C, van der Beek PA, Spiegel C (2011a) Episodic exhumation and relief growth in the Mont Blanc massif, western Alps from numerical modeling of thermochronology data. Earth Planet Sci Lett 304:417–430

Glotzbach C, Bernet M, van der Beek P (2011b) Detrital thermochronology records changing source areas and steady exhumation in the western european alps. Geology 39(3):239–242

Haeuselmann P, Granger DE, Jeannin PY (2007) Abrupt glacial valley incision at 0.8 Ma dated from cave deposits in Switzerland. Geology 35(2):143–146

Harkins N, Kirby E, Heimsath A, Robinson R, Reiser U (2007) Transient fluvial incision in the headwaters of the Yellow river, northeastern Tibet, China. J Geophys Res 112(F3). https://doi.org/10.1029/2006jf000570

Herman F, Copeland P, Avouac J-P, Bollinger L, Mahéo G, Le Fort P, Rai S, Foster D, Pêcher A, Stüwe K, Henry P (2010) Exhumation, crustal deformation, and thermal structure of the Nepal Himalaya derived from the inversion of thermochronological and thermobarometric data and modeling of the topography. J Geophys Res 115(B6). https://doi.org/10.1029/2008jb006126

Hetzel R, Dunkl I, Haider V, Strobl M, von Eynatten H, Ding L, Frei D (2011) Peneplain formation in southern Tibet predates the India-Asia collision and plateau uplift. Geology 39(10):983–986

House MA, Wernicke BP, Farley KA, Dumitru TA (1997) Cenozoic thermal evolution of the central Sierra Nevada, California, from (U–Th)/He thermochronometry. Earth Planet Sci Lett 151:167–179

House MA, Wernicke BP, Farley KA (1998) Dating topography of the Sierra Nevada, California, using apatite (U–Th)/He ages. Nature 396:66–69. https://doi.org/10.1038/23926

House MA, Wernicke BP, Farley KA (2001) Paleogeomorphology of the Sierra Nevada, California, from (U–Th)/He ages in apatite. Am J Sci 301:77–102

Hurford AJ (1986) Cooling and uplift patterns in the Lepontine alps, south central Switzerland, and an age of vertical movement on the insubric fault line. Contrib Mineral Petrol 92:413–427

Hurford AJ, Hunziker JC, Stöckhert B (1991) Constraints on the late thermotectonic evolution of the western Alps: evidence for episodic rapid uplift. Tectonics 10(4):758–769

Jamieson RA, Beaumont C (1988) Orogeny and metamorphism: a model for deformation and *P-T-t* paths with applications to the central and southern Appalachians. Tectonics 7:417–445

Karlstrom K, Crow R, McIntosh W, Peters L, Pederson J, Raucci J, Crossey LJ, Umhoefer P, Dunbar N (2007) $^{40}Ar/^{39}Ar$ and field studies of Quaternary basalts in Grand Canyon and model for carving Grand Canyon: quantifying the interaction of river incision and normal faulting across the western edge of the Colorado plateau. Geol Soc Am Bull 119:1283–1312

Karlstrom KE, Crow R, Crossey LJ, Coblentz D, van Wijk J (2008) Model for tectonically driven incision of the younger than 6 Ma Grand Canyon. Geology 31:835–838

Karlstrom KE, Lee JP, Kelley SA, Crow RS, Crossey LJ, Young RA, Lazear G, Beard LS, Ricketts JW, Fox M, Shuster DL (2014) Formation of the Grand Canyon 5 to 6 million years ago through integration of older palaeocanyons. Nature Geosci 7(3):239–244

Kirby E, Reiners PW, Krol MA, Whipple KX, Hodges KV, Farley KA, Tang W, Chen Z (2002) Late Cenozoic evolution of the eastern margin of the Tibetan plateau: inferences from $^{40}Ar/^{39}Ar$ and (U–Th)/He thermochronology. Tectonics 21(1):1001

Landry KR, Coutand I, Whipp DM Jr, Grujic D, Hourigan JK (2016) Late Neogene tectonically driven crustal exhumation of the Sikkim Himalaya: insights from inversion of multithermochronologic data. Tectonics 35(3):833–859

Larsen IJ, Montgomery DR (2012) Landslide erosion coupled to tectonics and river incision. Nat Geosci 5:468–473

Liu T-K, Hsieh S, Chen Y-G, Chen W-S (2001) Thermo-kinematic evolution of the Taiwan oblique-collision mountain belt as revealed by zircon fission track dating. Earth Planet Sci Lett 186:45–56

Lucchitta I (1972) Early history of the Colorado river in the basin and range province. Geol Soc Am Bull 83:1933–1948

Malusà MG, Fitzgerald PG (2018) Chapter 8. From cooling to exhumation: setting the reference frame for the interpretation of thermochronologic data. In: Malusà MG, Fitzgerald PG (eds) Fission-track thermochronology and its application to geology. Springer

Malusà MG, Fitzgerald PG (2018) Chapter 10. Application of thermochronology to geologic problems: bedrock and detrital approaches. In: Malusà MG, Fitzgerald PG (eds) Fission-track thermochronology and its application to geology. Springer

Malusà MG, Garzanti E (2018) Chapter 7. The sedimentology of detrital thermochronology. In: Malusà MG, Fitzgerald PG (eds) Fission-track thermochronology and its application to geology. Springer

Malusà MG, Resentini A, Garzanti E (2016) Hydraulic sorting and mineral fertility bias in detrital geochronology. Gondwana Res 31:1–19

Mancktelow NS, Grasemann B (1997) Time-dependent effects of heat advection and topography on cooling histories during erosion. Tectonophysics 270:167–195

Matmon A, Bierman PR, Larsen J, Southworth S, Pavich M, Caffee M (2003) Temporally and spatially uniform rates of erosion in the southern Appalachian great smoky mountains. Geology 31(2):155–158

McPhillips D, Brandon MT (2012) Topographic evolution of the Sierra Nevada measured directly by inversion of low-temperature thermochronology. Am J Sci 312:90–116

Miller SR, Slingerland RL, Kirby E (2007) Characteristics of steady state fluvial topography above fault-bend folds. J Geophys Res 112 (F4). https://doi.org/10.1029/2007jf000772

Montero-López C, Strecker MR, Schildgen TF, Hongn F, Guzmán S, Bookhagen B, Sudo M (2014) Local high relief at the southern margin of the Andean plateau by 9 Ma: evidence from ignimbritic valley fills and river incision. Terra Nova 26(6):454–460

Montgomery DR, Brandon MT (2002) Topographic controls on erosion rates in tectonically active mountain ranges. Earth Planet Sci Lett 201(3–4):481–489

Moon S, Chamberlain CP, Blisniuk K, Levine N, Rood DH, Hilley GE (2011) Climatic control of denudation in the deglaciated landscape of the Washington cascades. Nat Geosci 4:469–473

Moore MA, England PC (2001) On the inference of denudation rates from cooling ages of minerals. Earth Planet Sci Lett 185:265–284

Mulch A (2016) Stable isotope paleoaltimetry and the evolution of landscapes and life. Earth Planet Sci Lett 433(1):180–191

Muttoni G, Carcano C, Garzanti E, Ghielmi M (2003) Onset of major Pleistocene glaciations in the Alps. Geology 31(11):989–992

Olen SM, Ehlers TA, Densmore MS (2012) Limits to reconstructing paleotopography from thermochronometer data. J Geophys Res 117:F01024

Ouimet W, Whipple KX, Granger DE (2009) Beyond threshold hillslopes: channel adjustment to base-level fall in tectonically active mountain ranges. Geology 37(7):579–582

Ouimet W, Whipple K, Royden L, Reiners P, Hodges K, Pringle M (2010) Regional incision of the eastern margin of the Tibetan plateau. Lithosphere 2(1):50–63

Pederson J, Karlstrom KE, Sharp W, McIntosh W (2002) Differential incision of the Grand Canyon related to Quaternary faulting—constraints from U-series and Ar/Ar dating. Geology 30(8):739–742

Polyak V, Hill C, Asmerom Y (2008) Age and evolution of the Grand Canyon revealed by U-Pb dating of water table-type speleothems. Science 321:1377–1380

Reiners PW, Brandon MT (2006) Using thermochronology to understand orogenic erosion. Annu Rev Earth Planet Sci 34:419–466

Reiners PW, Ehlers TA, Mitchell SG, Montgomery DR (2003a) Coupled spatial variations in precipitation and long-term erosion rates across the Washington cascades. Nature 426:645–647

Reiners PW, Zhou Z, Ehlers TA, Xu C, Brandon MT, Donelick RA, Nicolescu S (2003b) Post-orogenic evolution of the Dabie Shan, eastern China, from (U–Th)/He and fission-track thermochronology. Am J Sci 303(6):489–518

Robert X, van der Beek P, Braun J, Perry C, Dubille M, Mugnier J-L (2009) Assessing Quaternary reactivation of the main central thrust zone (central Nepal Himalaya): new thermochronologic data and numerical modeling. Geology 37(8):731–734

Robert X, van der Beek P, Braun J, Perry C, Mugnier J-L (2011) Control of detachment geometry on lateral variations in exhumation rates in the Himalaya: insights from low-temperature thermochronology and numerical modeling. J Geophys Res 116(B5)

Roe GH, Montgomery DR, Hallet B (2003) Orographic precipitation and the relief of mountain ranges. J Geophys Res 108:2315

Rohrmann A, Kapp P, Carrapa B, Reiners PW, Guynn J, Ding J, Heizler M (2012) Thermochronologic evidence for plateau formation in central Tibet by 45 Ma. Geology 40(2):187–190

Ruddiman WF (ed) (1997) Tectonic uplift and climate change. Plenum, New York, p 535

Ruhl KW, Hodges KV (2005) The use of detrital mineral cooling ages to evaluate steady state assumptions in active orogens: an example from the central Nepalese Himalaya. Tectonics 24(4):TC4015

Schildgen TF, Hodges KV, Whipple KX, Reiners PW, Pringle MS (2007) Uplift of the western margin of the Andean plateau revealed from canyon incision history, southern Peru. Geology 35:523–526

Schildgen TF, Ehlers TA, Whipp DM Jr, van Soest MC, Whipple KX, Hodges KV (2009) Quantifying canyon incision and Andean plateau surface uplift, southwest Peru: a thermochronometer and numerical modeling approach. J Geophys Res 114:F04014

Schildgen TF, Balco G, Shuster DL (2010) Canyon incision and knickpoint propagation recorded by apatite $^{4}He/^{3}He$ thermochronometry. Earth Planet Sci Lett 293:377–387

Shuster DL, Farley KA (2004) ^{4}He/^{3}He thermochronometry. Earth Planet Sci Lett 217:1–17

Shuster DL, Farley KA (2005) ^{4}He/^{3}He thermochronometry: theory, practice, and potential complications. Rev Mineral Geochem 58:181–203

Shuster DL, Ehlers TA, Rusmore ME, Farley KA (2005) Rapid glacial erosion at 1.8 Ma revealed by ^{4}He/^{3}He thermochronometry. Science 310:1668–1670

Shuster DL, Cuffey KM, Sanders JW, Balco G (2011) Thermochronometry reveals heaward propagation of erosion in an alpine landscape. Science 332:84–88

Simon-Labric T, Brocard GY, Teyssier C, van der Beek P, Reiners PW, Shuster DL, Murray KE, Whitney DL (2014) Low-temperature thermochronologic signature of range-divide migration and breaching in the north cascades. Lithosphere 6(6):473–482

Spotila JA (2005) Applications of low-temperature thermochronometry to quantification of recent exhumation in mountain belts. Rev Mineral Geochem 58:449–466

Stock GM, Anderson RS, Finkel RC (2004) Pace of landscape evolution in the Sierra Nevada, California, revealed by cosmogenic dating of cave sediments. Geology 32:193–196

Stüwe L, White R, Brown X (1994) The influence of eroding topography on steady-state isotherms; application to fission-track analysis. Earth Planet Sci Lett 124:63–74

Thouret J-C, Wörner G, Gunnell Y, Singer B, Zhang X, Souriot T (2007) Geochronologic and stratigraphic constraints on canyon incision and Miocene uplift of the central Andes in Peru. Earth Planet Sci Lett 263(3–4):151–166

Valla PG, Herman F, van der Beek PA, Braun J (2010) Inversion of thermochronological age-elevation profiles to extract independent estimates of denudation and relief history—I: theory and conceptual model. Earth Planet Sci Lett 295:511–522

Valla PG, Shuster DL, van der Beek PA (2011) Significant increase in relief of the European Alps during mid-Pleistocene glaciations. Nat Geosci 4:688–692

van der Beek P, van Melle J, Guillot S, Pêcher A, Reiners PW, Nicolescu S, Latif M (2009) Eocene Tibetan plateau remnants preserved in the northwest Himalaya. Nat Geosci 2:364–368

van der Beek PA, Valla P, Herman F, Braun J, Persano C, Dobson KJ, Labrin E (2010) Inversion of thermochronological age-elevation profiles to extract independent estimates of denudation and relief

history—II: application to the French Western Alps. Earth Planet Sci Lett 296:9–22

van der Beek P, Litty C, Baudin M, Mercier J, Robert X, Hardwick E (2016) Contrasting tectonically driven exhumation and incision patterns, western versus central Nepal Himalaya. Geology 44 (4):327–330

Wagner GA, Reimer GM (1972) Fission track tectonics: the tectonic interpretation of fission track ages. Earth Planet Sci Lett 14:263–268

Wagner GA, Reimer GM, Jäger E (1977) Cooling ages derived by apatite fission track, mica Rb-Sr, and K-Ar dating: the uplift and cooling history of the central Alps. Mem Inst Geol Mineral Univ Padova 30:1–27

Wernicke B (2011) The California river and its role in carving Grand Canyon. Geol Soc Am Bull 123:1288–1316

Whipp DM Jr, Ehlers TA, Blythe AE, Huntington KW, Hodges KV, Burbank DW (2007) Plio-Quaternary exhumation history of the central Nepalese Himalaya: 2. thermokinematic and thermochronometer age prediction model. Tectonics 26(3)

Whipple KX, Tucker GE (1999) Dynamics of the stream-power river incision model: implications for height limits of mountain ranges, landscape response timescales, and research needs. J Geophys Res 104:17661–17674

Willett SD (1999) Orogeny and orography: the effects of erosion on the structure of mountain belts. J Geophys Res 104:28957–28981

Willett SD, Brandon MT (2002) On steady states in mountain belts. Geology 30(2):175–178

Willett SD, Slingerland R, Hovius N (2001) Uplift, shortening, and steady state topography in active mountain belts. Am J Sci 301:455–485

Willett SD, Fisher D, Fuller C, En-Chao Y, Chia-Yu L (2003) Erosion rates and orogenic-wedge kinematics in Taiwan inferred from fission-track thermochronology. Geology 31(11):945–948

Wolf RA, Farley KA, Kass DM (1998) Modeling of the temperature sensitivity of the apatite (U–Th)/He thermochronometer. Chem Geol 148:105–114

Yang R, Fellin MG, Herman F, Willett SD, Wang W, Maden C (2016) Spatial and temporal pattern of erosion in the three rivers region, southeastern Tibet. Earth Planet Sci Lett 433:10–20

Zeitler PK, Johnson NM, Naeser CW, Tahirkheli RAK (1982) Fission-track evidence for Quaternary uplift of the Nanga Parbat region, Pakistan. Nature 298:255–257